THIN FILM DIAMOND

EDITED BY A. LETTINGTON AND J.W. STEEDS

The Royal Society

CHAPMAN & HALL

SHED BY CHAPMAN & HALL FOR THE ROYAL SOCIETY

Thin Film Diamond

Edited by A. Lettington and J.W. Steeds

Published by Chapman & Hall for The Royal Society

The Royal Society

CHAPMAN & HALL
London · Glasgow · New York · Tokyo · Melbourne · Madras

Published by Chapman & Hall, 2–6 Boundary Row, London SE1 8HN

Chapman & Hall, 2–6 Boundary Row, London SE1 8HN, UK

Blackie Academic & Professional, Wester Cleddens Road, Bishopbriggs, Glasgow G64 2NZ, UK

Chapman & Hall Inc., One Penn Plaza, 41st Floor, New York NY 10119, USA

Chapman & Hall Japan, Thomson Publishing Japan, Hirakawacho Nemoto Building, 6F, 1-7-11 Hirakawa-cho, Chiyoda-ku, Tokyo 102, Japan

Chapman & Hall Australia, Thomas Nelson Australia, 102 Dodds Street, South Melbourne, Victoria 3205, Australia

Chapman & Hall India, R. Seshadri, 32 Second Main Road, CIT East, Madras 600 035, India

First edition 1994

Typeset by Thomson Press, India
Printed in Great Britain by the University Press, Cambridge

ISBN 0 412 49630 5

A catalogue record for this book is available from the British Library

Library of Congress Cataloging-in-Publication data
Thin film diamonds / edited by A. Lettington and J.W. Steeds. – 1st ed.
p. cm.
Includes index.
ISBN 0-412-49630-5
1. Diamonds, Artificial. 2. Diamond thin films. I. Lettington, Alan H. II. Steeds, J. W. III. Royal Society (Great Britain)
TP873.5.D5T47 1994
666.88–dc20 93-33950
CIP

Printed on permanent acid-free text paper, manufactured in accordance with the proposed ANSI/NISO Z39.48-1992 and ANSI/NISO Z39.48-1984 (Permanence of Paper).

Contributors

T. Ando National Institute for Research in Inorganic Materials, 1-1 Namiki, Tsukuba, Ibaraki 305, Japan

John C. Angus Department of Chemical Engineering, Case Western Reserve University, Cleveland, Ohio 44106, USA

T. R. Anthony GE Research & Development Center, P.O. Box 8, Schenectady, New York 12309, USA

Alberto Argoitia Department of Chemical Engineering, Case Western Reserve University, Cleveland, Ohio 44106, USA

Peter K. Bachmann Philips Research Laboratories, Solid Films and Deposition Technologies, P.O. Box 1980, D-5100 Aachen, Germany

James E. Butler Code 6174, Naval Research Laboratory, Washington, DC 20375-5000, USA

C.D. Clark J. J. Thomson Physical Laboratory, University of Reading, Whiteknights, Reading RG6 2AF, UK

Alan T. Collins Wheatstone Physics Laboratory, King's College London, Strand, London WC2R 2LS, UK

C. B. Dickerson J. J. Thomson Physical Laboratory, University of Reading, Whiteknights, Reading RG6 2AF, UK

Z. Feng Computer Mechanics Laboratory, University of California at Berkeley, USA

J. E. Field Cavendish Laboratory, Madingley Road, Cambridge CB3 0H3, UK

H. Fujita Central Research Laboratory, Onoda Cement Co. Ltd, 2-2-1 Ishikawa, Sakura, Chiba 285, Japan

Roy Gat Department of Chemical Engineering, Case Western Reserve University, Cleveland, Ohio 44106, USA

R. Haubner Technical University Vienna, Institute for Chemical Technology of Inorganic Materials, Getreidemarkt 6/161, A-1060 Vienna, Austria

M. Kamo National Institute for Research in Inorganic Materials, 1-1 Namiki, Tsukuba, Ibaraki 305, Japan

Alan H. Lettington J. J. Thomson Physical Laboratory, University of Reading, Whiteknights, Reading RG6 2AF, UK

Zhidan Li Department of Chemical Engineering, Case Western Reserve University, Cleveland, Ohio 44106, USA

B. Lux Technical University Vienna, Institute for Chemical Technology of Inorganic Materials, Getreidemarkt 6/161, A-1060 Vienna, Austria

E. Nicholson Cavendish Laboratory, Madingley Road, Cambridge CB3 0HE, UK

J. Robertson National Power Labs, Leatherhead, Surrey KT22 7SE, UK

Y. Sato National Institute for Research in Inorganic Materials, 1-1 Namiki, Tsukuba, Ibaraki 305, Japan

M. Seal Sigillum B.V., P.O. Box 7129, Amsterdam 1007 JC, The Netherlands

C. R. Seward Cavendish Laboratory, Madingley Road, Cambridge CB3 0HE, UK

Mahendra Sunkara Department of Chemical Engineering, Case Western Reserve University, Cleveland, Ohio 44106, USA

T. Tanaka National Institute for Research in Inorganic Materials, 1-1 Namiki, Tsukuba, Ibaraki 305, Japan

Long Wang Department of Chemical Engineering, Case Western Reserve University, Cleveland, Ohio 44106, USA

Yaxin Wang Department of Chemical Engineering, Case Western Reserve University, Cleveland, Ohio 44106, USA

Richard L. Woodin Norton Diamond Film, Northboro, Massachusetts 01532-1545, USA

Preface

This volume contains a selection of invited review papers presented at a Royal Society Discussion meeting on Thin Film Diamond held in London on 15 and 16 July 1992.

The topic of low pressure synthesis has attracted world wide interest and become increasingly active in recent years due to the possible use of diamond films in commercial applications.

Until recently commercial diamond synthesis was almost entirely by the high pressure high temperature technique in which diamond is precipitated as an equilibrium phase from a carbon-containing liquid metal catalyst. In this way crystals may be formed up to 10mm or so in size. The metastable low pressure techniques cannot compete in cost but can be used to fabricate large area wafers or predetermined shapes not possible by other means.

Most of the low pressure techniques stem from the work of Eversole which was first reported in 1962. He exposed a hot diamond substrate alternately to a hydrocarbon gas, which deposited a mixture of diamond and graphite, and then to hydrogen, which preferentially etched away the graphite. In later developments these two stages have been combined to form a continuous process and differ only in the way the etchant is generated. In this volume an historical overview of these low pressure growth techniques and a description of diamond and crystal morphology is given by John Angus and his co-authors in their paper on the chemical vapour deposition of diamond. James Butler and Richard Woodin discuss the kinetics and gas phase chemistry involved in thin film growth and Peter Bachmann reviews the current deposition techniques. He also summarizes the results of various deposition conditions and shows that diamond growth is possible only in a narrow range of gas compositions. Y. Sato and co-workers report on the local epitaxial growth of diamond on nickel substrates.

Other papers discuss the electronic, optical, thermal and mechanical properties of thin diamond films. The relationship between diamond and diamond-like carbon (DLC) is now better understood and this volume also contains papers on the electronic structure, deposition techniques and applications of DLC films.

The final paper in this volume discusses the various thermal and optical infrared and X-ray applications of diamond thin films. They have also been used in cutting and grinding and as the active element in semiconducting devices.

The subject is advancing rapidly, with many patents being taken out each year. It is nevertheless an opportune time to review the field since there is much fundamental and applied research that needs to be undertaken before this topic can realize its full potential. It is hoped that this volume will provide a valuable overview of thin film diamond for years to come.

A. H. LETTINGTON
J. W. STEEDS

Contents

1

Chemical vapour deposition of diamond

BY JOHN C. ANGUS, ALBERTO ARGOITIA, ROY GAT, ZHIDAN LI, MAHENDRA SUNKARA, LONG WANG AND YAXIN WANG

Growth of diamond at conditions where it is the metastable phase can be achieved by various chemical vapour deposition methods. Atomic hydrogen plays a major role in mediating rates and in maintaining a proper surface for growth. Low molecular weight hydrocarbon species (e.g. CH_3 and C_2H_x) are believed to be responsible for extension of the diamond lattice, but complete understanding of attachment mechanisms has not yet been achieved. The nucleation of diamond crystals directly from the gas phase can proceed through a graphitic intermediate. Once formed, the growth rate of diamond crystals is enhanced by the influence of stacking errors. Many of the commonly observed morphologies, e.g. hexagonal platelets and (apparent) decahedral and icosahedral crystals, can be explained by the influence of simple stacking errors on growth rates. *In situ* measurements of growth rates as a function of hydrocarbon concentration show that the mechanism for diamond growth is complex and may involve surface adsorption processes in rate limiting steps. The transport régime in diamond deposition reactors varies widely. In the hot-filament and microwave reactors, which operate from 20 to 100 Torr (1 Torr $\approx$ 133 Pa), the transport of mass and energy is dominated by molecular diffusion. In the atmospheric pressure combustion and plasma methods, transport is dominated by convection. *In situ* measurements of H atom recombination rates in hot-filament reactors show that, under many commonly used process conditions, transport of atomic hydrogen to the growing surface is diffusion limited and H atom recombination is a major contributor to energy transport.

1. Introduction

Diamond synthesis by chemical vapour deposition (CVD), at pressures and temperatures where diamond is metastable with respect to graphite, was first achieved by William G. Eversole of the Union Carbide Corporation (Eversole 1962). Unpublished reports show that Eversole achieved growth of new diamond during the period 26 November 1952 to 7 January 1953 (A. D. Kiffer). This is just before 15 February 1953, the date of the first high-pressure–high-temperature synthesis of diamond by Liander & Lundblad (1960) at Allemana Svenska Eliktriska Aktiebolaget (ASEA), and well ahead of the synthesis by General Electric in 1954.

Efforts to grow diamond at low pressures arose independently of each other and without knowledge of the Eversole work in both the Soviet Union and the United States (Spitsyn & Deryagin 1956; Angus 1961). The first published papers from these groups did not appear until much later (Angus *et al.* 1968; Deryagin *et al.* 1968). The use of atomic hydrogen to etch graphitic deposits (Angus *et al.* 1971) and its use during growth to permit high rate nucleation and growth of diamond on non-

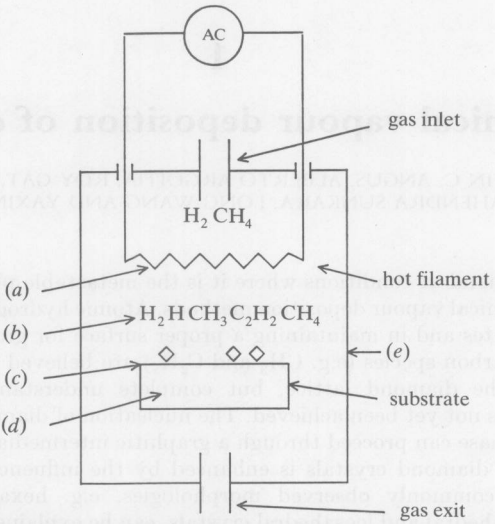

Figure 1. Schematic diagram of hot-filament chemical vapour deposition reactor (permission of *A. Rev. Mater. Sci.*). Reaction numbers refer to table 1. (*a*) Reaction 1; (*b*) gas phase reactions 2–6; (*c*) surface reactions 7–9; (*d*) solid state diffusion, carbide formation; (*e*) wall reactions.

diamond substrates (Deryagin *et al.* 1976) followed. The current intense level of interest can be traced to the Japanese group at the National Institute for Research in Inorganic Materials (NIRIM) in Tsukuba, Japan. They revealed details of several methods for the CVD of diamond, including the widely used hot-filament and microwave plasma assisted techniques (Matsumoto *et al.* 1982*a*, *b*; Kamo *et al.* 1983; Matsui *et al.* 1983).

Details of the history of diamond synthesis have been extensively reported elsewhere and will not be repeated here (Davies 1984; DeVries 1987; Badzian & DeVries 1988; Angus 1989, 1990).

Diamond has long been known to be thermodynamically stable with respect to graphite only at high pressure (Leipunski 1939; Berman & Simon 1955). This fact was erroneously interpreted by many workers to mean that diamond could never be synthesized at low pressures, where graphite is the stable form of carbon. A notable exception to this view was Bridgman (1955).

Diamond is, in fact, only slightly unstable with respect to graphite. At 298 K and 1 atm† pressure, the difference in free energy between diamond and graphite is only 2.900 kJ mol^{-1} (approximately 0.03 eV per atom), which is only on the order of kT. Furthermore, there is a very large activation barrier inhibiting the transformation of diamond to graphite. Of perhaps more significance is the fact that graphite (2.26 g cm^{-3}) is less dense than diamond (3.51 g cm^{-3}). Therefore as solid carbon precipitates out of a supersaturated carbon gas, the 'first' phase encountered is graphite, not diamond. This is an example of Volmer's rule, which states that the least dense solid phase is the first to crystallize from a supersaturated fluid phase. Once formed, graphite will not spontaneously transform further into diamond

because it is the stable phase and because of the high activation barrier between the two phases. However, atomic hydrogen changes the relative energies of small graphitic and diamond nuclei and provides a means for circumventing the large activation barrier. This will be discussed in more detail in §3 below.

In CVD of diamond from C/H and C/H/O gas mixtures the gas phase is decomposed to atomic hydrogen, molecular fragments, free radicals and sometimes ions. The most commonly used methods are various types of plasma discharges, heated filaments and combustion. Diamond is formed from these complex gas phase reaction mixtures on substrates held at nominal temperatures from 700 °C to 1000 °C. A simple schematic of a hot-filament reactor is shown in figure 1. Although details of the complex reaction and transport processes are still the subject of much research, a general understanding of the reactor environment and the principal reactions and energy flows has been achieved.

2. Diamond growth

Some of the principal reactions of importance are summarized in table 1 with an estimate of their standard enthalpy and free energy changes. Examination of table 1 gives a clear picture of the basic energetics of the entire diamond deposition process. The principal function of the hot filament, or equivalently the plasma discharge, is to provide large amounts of atomic hydrogen through the decomposition of molecular hydrogen (reaction 1). This reaction has a very positive enthalpy change.

The atomic hydrogen, once formed, undergoes several spontaneous, highly exothermic, reactions. It can react with hydrocarbons in the gas phase, abstracting hydrogen to form methyl radicals (reaction 2). Recombination of atomic hydrogen to form molecular hydrogen (reaction 3) is also possible. However, since this is a three body reaction, its rate is slow at low reactor pressures and often can be ignored despite the favourable free energy change. Methyl radical destruction can take place by recombination with atomic hydrogen (reaction 4) or by diffusion out of the reaction zone to the walls of the reactor. There are gas phase reaction paths to higher molecular weight species, e.g. reaction 5. A spectrum of C_2H_x species can be formed by subsequent hydrogen atom abstraction reactions of the general type shown in reaction 6. These can lead to still higher molecular weight compounds by subsequent reactions not shown in table 1.

Atomic hydrogen will hydrogenate a bare diamond surface (reaction 7). Hydrogenated diamond surfaces are less prone to surface reconstruction than bare surfaces. On (111) surfaces, for example, bonded hydrogen helps maintain the bulk terminated diamond surface structure (Lander & Morrison 1964). Hydrogen can also abstract hydrogen from a hydrogen covered surface (reaction 8). This reaction is thermodynamically favoured because of the strong H–H bond. At typical substrate temperatures the fractional coverage is dominated by the competition between reactions 7 and 8. To first order, the steady state concentration of free radical sites, f_s, is independent of the atomic hydrogen concentration and is approximately given by the competition between reactions 7 and 8

$$f_s = k_8/(k_7 + k_8), \tag{1}$$

where k_7 and k_8 are the first order rate constants for reactions 7 and 8. f_s can be estimated using kinetic constants for analogous gas phase reactions. At temperatures

Table 1. *Standard enthalpy and free energy changes of some important reactions during diamond growth*

(1 kcal = 4.184 kJ.)

	reaction	T/(K)	ΔH^0/(kcal mol^{-1})	ΔG^0/(kcal mol^{-1})[a]
	on filament			
1	$H_2 \rightarrow 2H$	2500	+109	+37[b]
	in gas phase			
2	$H + CH_4 \rightarrow CH_3 + H_2$	1800	*ca.* 0	−11
3	$H + H + M \rightarrow H_2 + M$	1800	−108	−57
4	$CH_3 + H + M \rightarrow CH_4 + M$	1800	−108	−45
5	$CH_3 + CH_3 + M \rightarrow C_2H_6 + M$	1800	−86[c]	−26[c]
6	$C_2H_x + H \rightarrow C_2H_{x-1} + H_2$	1800	small	small
	on substrate (S)			
7	$H + S \rightarrow S{-}H$	1200	−94	−68
8	$S{-}H + H \rightarrow S + H_2$	1200	−13	−6
9	$CH_3 + S \rightarrow S{-}CH_3$	1200	−81	−47

[a] Rossini & Jessup (1938), Stull *et al.* (1969) and Stull & Prophet (1971).
[b] At 20 Torr and 2500 K, the equilibrium mole fraction of atomic H is 0.16.
[c] Molecular mechanics estimate.

of 1000 and 1750 K, f_s was estimated to be 0.12 and 0.37 respectively (Kuczmarski 1992). These sites are where free radicals such as CH_3 (reaction 9) or acetylenic species, C_2H_x, can add to the surface. Finally, the H atom recombination on the surface contributes substantially to the energy flux delivered to the substrate. The recombination could be direct through reaction 3 where the surface plays the role of the third body or it could result as the net reaction from the two step process of reactions 7 and 8.

Much attention has focused on identification of the gas phase 'growth species' that are responsible for the addition of carbon to the diamond surface. Methyl radical, CH_3, and acetylene, C_2H_2, are believed to be the most likely candidates. Recent evidence, for example the isotope labelling studies of Chu *et al.* (1991) indicate that the methyl radical is the primary source of added carbon. The state of understanding has been the subject of an excellent recent review by Celii & Butler (1991) in which they summarized the extensive studies of Tsuda, Frenklach, Harris, Hauge and others. A recent molecular dynamics study by Garrison *et al.* (1992) of growth on the diamond (001) surface is also of great interest.

Recent microbalance studies of diamond growth kinetics show a complex behaviour. In a hot-filament reactor at 20 Torr†, the growth rate of diamond was first order in methane from 0.1% to 1.0% CH_4 (Wang *et al.* 1992). At high methane concentrations, the reaction tended to zero order. For the two-carbon source gases, C_2H_2, C_2H_4 and C_2H_6, the reaction was approximately one half order for concentrations from 0.3% to 1.0% hydrocarbon. Below a concentration of 0.3% hydrocarbon, the two-carbon gases showed a first order rate (see figure 2). The data are in agreement with a much earlier study (Chauhan *et al.* 1976) in which first-order kinetics were found for CH_4 and half order for C_2H_4. These data can be rationalized by mechanisms that involve single-carbon atom species in rate limiting steps. The zero-order dependence on CH_4 at high concentrations may arise from adsorbed intermediates.

† 1 Torr ≈ 133 Pa.

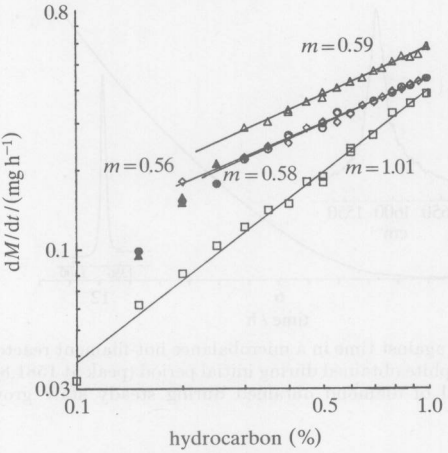

Figure 2. Log reaction rate against mole hydrocarbon (%) for various C_1 and C_2 gases. □, CH_4; ◇, C_2H_2; ○, C_2H_4; △, C_2H_6.

3. Diamond nucleation

The spontaneous nucleation of new diamond crystals under conditions where graphite is the stable carbon phase has been difficult to rationalize. Matsumoto & Matsui (1983) proposed, on the basis of symmetry arguments, that hydrocarbon cage compounds might serve as diamond precursors. It was proposed that a more likely precursor for diamond nucleation would be graphitic intermediates, which are subsequently hydrogenated by atomic hydrogen to saturated structures that can act as sites for diamond growth (Angus *et al.* 1988; Sunkara *et al.* 1990). Recent experimental studies support this latter view. Belton & Schmieg (1990) studied the nature of carbon bonding at different stages of nucleation on platinum substrates using X-ray photoelectron spectroscopy. They found that a carbon phase with graphitic bonding first formed, followed by a hydrogenated carbon phase and finally diamond. Microbalance studies of diamond nucleation and growth on platinum (Wang *et al.* 1992) show an initial induction period in which an oriented graphite deposit forms. Subsequently, this deposit disappears and the final deposit contains only polycrystalline diamond. A plot of the mass against time data and the observed Raman signals are shown in figure 3.

The nature of diamond nucleation can be probed by using graphite flakes as seed crystals. If the graphite is acting as a true nucleation site and not simply as an extra source of carbon, one would expect to find an orientational relation between the diamond and the original graphite substrate. Initial experiments on diamond growth on graphite seed crystals showed that the (111) diamond plane was parallel to the basal (0001) plane of the graphite (Angus *et al.* 1991). Subsequent experiments show that in addition to (111) diamond ∥ (0001) graphite, one often has a directional orientation within the planes, i.e. $[1\bar{1}0]$ diamond ∥ $[11\bar{2}0]$ graphite (Li *et al.* 1992). This relation means that the puckered six-membered rings in the diamond (111) planes retain the same orientation as the flat six-membered rings in the graphite basal (0001) plane. A transmission electron micrograph of one of these oriented

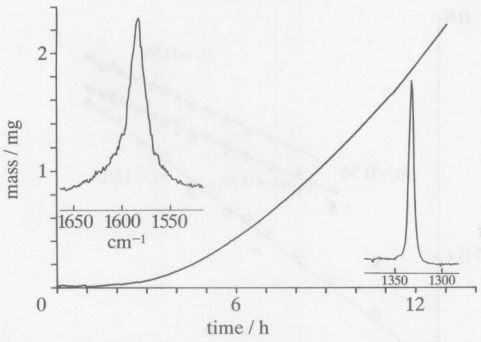

Figure 3. Mass of diamond against time in a microbalance hot-filament reactor. Inset at upper left shows Raman signal of graphite obtained during initial period (peak at 1581.8 cm^{-1}). Inset at lower right shows Raman signal of diamond obtained during steady state growth period (peak at 1333.1 cm^{-1}).

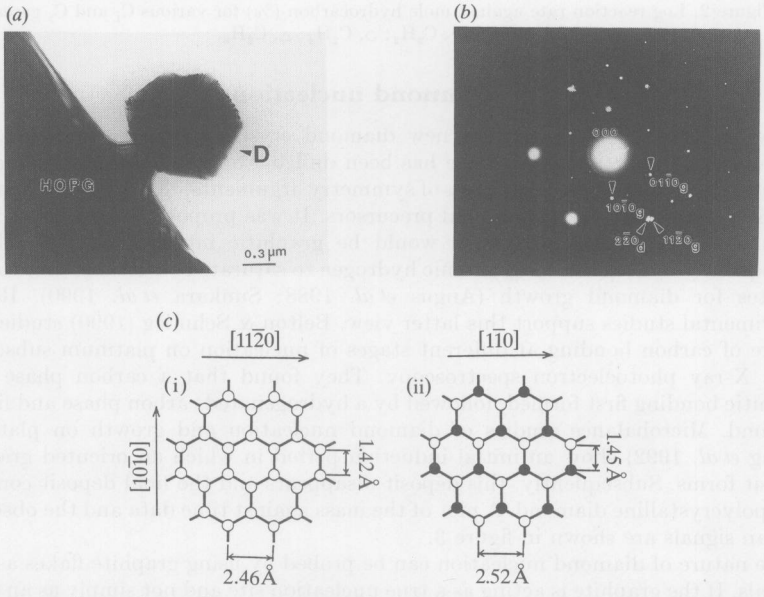

Figure 4. (*a*) Transmission electron micrograph of diamond nucleated on edge of highly oriented pyrolytic graphite. View is along normal to (0001) basal plane of graphite and the (111) plane of diamond. (*b*) Electron diffraction pattern from diamond and graphite shown in (*a*). (*c*) Orientation of (0001) graphite plane (i) and (111) diamond plane (ii).

diamond crystals on graphite, the corresponding diffraction pattern and the geometric relationship between the two structures are shown in figure 4.

The energetics of the conversion of graphitic, sp^2 bonded precursors can be examined by simple thermochemical calculations. Badziag *et al.* (1990) pointed out that hydrogen terminated 'diamonds' less than 3 nm in diameter have a lower

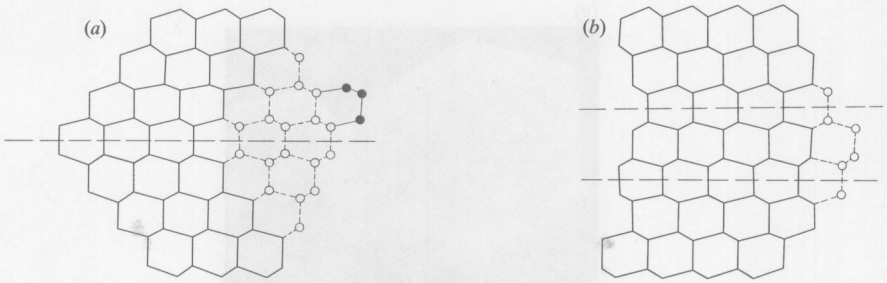

Figure 5. (*a*) ⟨110⟩ projection of diamond lattice containing one stacking error. Open circles and dashed lines show crystal filling out to smooth {111} surfaces with a convex corner. Three-atom nucleus shown on {111} surface with filled circles (permission *J. Mater. Res.*); (*b*) ⟨110⟩ projection of diamond lattice containing two stacking errors (extrinsic stacking fault). Open circles show crystal filling out to give a re-entrant (concave) corner. Two-atom nucleus shown with closed circles. Further growth can occur without the necessity of a three-atom nucleation event.

energy than hydrogen terminated graphite nuclei with the same number of carbon atoms. This means that in an environment rich in atomic hydrogen, the sp^3, tetrahedrally coordinated nuclei are in fact energetically favoured over the sp^2, trigonally coordinated nuclei. This work was subsequently criticized by Stein (1990), who pointed out that the correct parameter to consider is the free energy change for the appropriate reaction. However, Stein neglected to account for the fact that the active reagent under diamond growing conditions is atomic hydrogen, H, not molecular hydrogen, H_2. The enthalpy and free energy changes for the sequential hydrogenation of graphite to naphthalene and decalin by atomic hydrogen are:

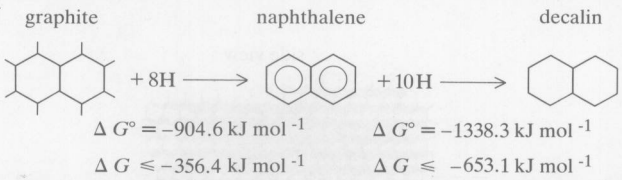

(ΔG was calculated from nominal reaction conditions of 0.01 atomic fraction of hydrogen, pressure of 20 Torr and equal activities of naphthalene, decalin and graphite. Data were taken from Stull *et al.* (1969).) The estimated free energy changes at reaction conditions are strongly negative for these model reactions, which shows that graphitic nuclei can indeed be converted into hydrogen saturated structures similar to diamond. Molecular orbital studies of the hydrogenation of single graphite sheets also support this conclusion (Angus *et al.* 1991; Mehandru *et al.* 1992). In addition, cyclopropane and cyclohexane are found as products when graphite is reacted with atomic hydrogen (Rye 1977). Other workers have also used thermodynamic methods to show that hydrogen stabilizes diamond surfaces (Sommer *et al.* 1989; Piekarcyk *et al.* 1989; Yarbrough *et al.* 1990; Harris *et al.* 1991).

The nucleation sequence may start with the formation of high molecular graphitic and polynuclear aromatic hydrocarbons (PAH) by the sequential polymerization of acetylene (Frenklach *et al.* 1985). These high molecular weight materials are sufficiently non-volatile so that they remain on the substrate until they become hydrogenated by atomic hydrogen, forming the saturated edge structure that is

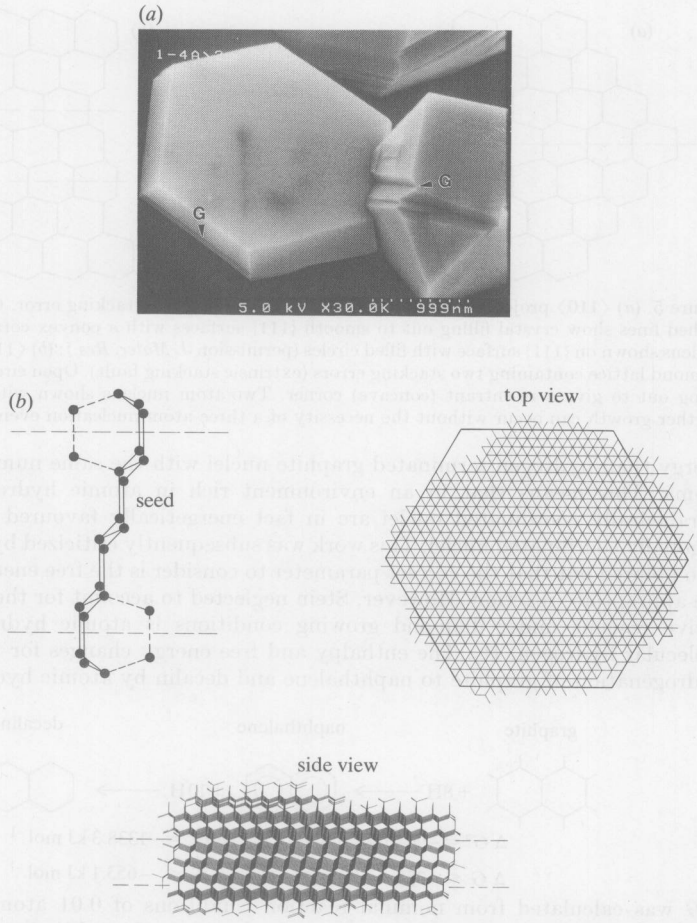

Figure 6. (*a*) Hexagonal diamond platelet and fully faceted three-dimensional diamond crystal. Re-entrant grooves are visible along the side faces of the hexagonal platelet and on the fully faceted crystal (marked with Gs). (*b*) Seed nucleus and top and side views of resulting hexagonal platelet grown by Monte Carlo simulation. Stacking errors are shown by dashed lines.

attractive for diamond nucleation. The atomic hydrogen plays a multiple role in this process. By terminating the dangling surface bonds it stabilizes the tetrahedrally coordinated, sp^3 nuclei with respect to the trigonally coordinated, sp^2 nuclei. It also serves as a reactive solvent which permits the conversion of graphitic nuclei into diamond nuclei, thereby circumventing the large activation barrier separating graphite from diamond. The mechanism is consistent with the careful observations of Lux, who showed that induction times for nucleation are shortest on those metals that can achieve a supersaturation of carbon on the surface the most rapidly (Joffreau *et al.* 1988; Lux & Haubner 1991).

Other methods of diamond nucleation are also possible. For example, growth

Table 2. *Relation of observed morphology to types of stacking errors during growth of {111} faceted crystals*

type of error	morphology
two stacking errors on parallel (111) planes (intrinsic or extrinsic stacking fault or micro twin)	hexagonal platelet
three stacking errors on parallel (111) planes	truncated hexagonal platelet
two stacking errors on non-parallel (111) planes	decahedral (pseudo five-fold symmetry)
three stacking errors on non-parallel (111) planes	icosahedral
single stacking error	triangular (macle)

on diamond debris left by scratching the substrate surface with diamond powder is commonly done (Iijima 1991).

The observed morphologies of vapour-grown diamond crystals range include: spherical clusters of diamond microcrystals, cubes, cubo-octahedrons, octahedrons and flat hexagonal platelets. Complex, multiply twinned forms (e.g. decahedrons and icosahedrons) are also observed. Twinned clusters, with many re-entrant surfaces, are perhaps the most common form, especially when in a regime that gives octahedral {111} faceting.

Defects that arise during growth can mediate further growth of the crystal. It appears that re-entrant corners play a major role in enhancing diamond growth rates. The re-entrants arise from the intersection of {111} twin bands or stacking faults with the surface. The re-entrant corners are favourable sites for nucleation of new layers. This effect has been known for many years in other contexts and was exploited for the rapid growth of silicon web from the melt. Presumably, the enhanced nucleation rate arises because only two atoms are required to form a stable nucleus at the re-entrant corner rather than three atoms that are required on a smooth {111} surface. This is shown schematically in figure 5. A recent discussion of the nucleation at re-entrant corners has been given by Tiller (1991).

Many complex morphologies can arise from the enhancement of growth rates by the re-entrant corners arising from multiple stacking errors (Sunkara 1992; Angus *et al.* 1991, 1992). A Monte Carlo computer program was used in which atoms were added to seed 'crystals' with different types of stacking errors (Sunkara 1992). A computer 'grown' hexagonal platelet and a scanning electron micrograph of a hexagonal diamond platelet are shown in figure 6. This morphology arises from the action of two parallel stacking errors. In the model shown in figure 6, the two stacking errors are separated by two layers of correct stacking. The growth rate within the plane of this microtwin is much greater than the growth rate normal to the plane because of the re-entrant corner on the periphery of the crystal. The result is a flat platelet of hexagonal shape and low aspect ratio. Hexagonal diamond platelets have been observed by several workers (Everson & Tamor 1991; Angus *et al.* 1991, 1992) and may reflect the nature of the precursor that leads to diamond nucleation. In a much earlier study, hexagonally shaped platelets of silver bromide were attributed to the mechanism described above (Berriman & Herz 1957).

Many other morphologies commonly observed in vapour-grown diamond can also be explained by the interaction of various combinations of stacking errors. These are summarized in table 2.

Table 3. *Comparison of mass and energy transport in diamond reactors*

type of reactor	Pe_{mass}	Pe_{thermal}
hot filaments	6×10^{-4}	8×10^{-4}
microwave	5×10^{-4}	7×10^{-3}
plasma torch	60	300
combustion	12	7

(Note that

$$Pe_{\text{mass}} = \frac{\langle u \rangle L}{D}\left[\frac{\text{mass flux by convection}}{\text{mass flux by diffusion}}\right],$$

$$Pe_{\text{thermal}} = \frac{\langle u \rangle L}{\alpha}\left[\frac{\text{thermal flux by convection}}{\text{thermal flux by diffusion}}\right],$$

where $\langle u \rangle$ is the average convective velocity, L is a characteristic length, D is the diffusion coefficient and α is the thermal diffusivity.)

4. Reactor environment

Much less attention has been paid to the transport processes within the reactor than to the attachment kinetics at the diamond surface. This is somewhat surprising since there is growing evidence that diamond growth rates may be limited by transport processes (Angus *et al.* 1989; Rau & Picht 1992). A complete understanding of diamond deposition must include a simultaneous solution of the energy and mass transport equations together with a detailed chemical mechanism. Simplified reactor models have been described (Debroy *et al.* 1990; Goodwin & Gavilett 1991; Kuczmarski *et al.* 1991). In the absence of a detailed reactor model, much of interest can be learned from an analysis of existing growth rate data.

A comparison of the transport of species and energy between the various types of reactors has been made (Angus *et al.* 1989, 1991). In the low pressure processes (e.g. microwave and hot-filament-assisted deposition) the transport is entirely dominated by molecular diffusion. Convection plays virtually no role. On the other hand, in the atmospheric pressure plasma torch and in atmospheric combustion, the transport is dominated by convection. An estimate of the magnitude of these effects can be obtained by computing average Peclet numbers. These results are shown in table 3. The growth rates in the atmospheric pressure, high gas velocity processes are much higher than in the low pressure processes. This is suggestive that the growth rate is limited by the rate of transport of species rather than by the attachment kinetics.

Similarly, the thermal Peclet numbers indicate that in typical hot-filament and microwave reactors, heat transport by conduction is much more important than heat transport by forced convection. The opposite is true in the plasma torch and combustion reactors.

The importance of natural convection in hot-filament reactors can be estimated from the Grashof number, Gr,

$$Gr = g\beta L^3 \Delta T/\nu^2, \tag{2}$$

where g is the acceleration of gravity, β the volumetric expansion coefficient, L a characteristic length, ΔT a temperature difference and ν the kinematic viscosity. The Grashof number is a measure of the relative magnitude of buoyancy forces to viscous